Variational Transition-State Theory Rate Constant Calculations of the OH + CH 3 SH Reaction and Several Isotopic Variants

ARTICLE *in* THE JOURNAL OF PHYSICAL CHEMISTRY A · JUNE 2003

Impact Factor: 2.69 · DOI: 10.1021/jp021744x

3 AUTHORS:

Laura Masgrau
Autonomous University of Barcelona
41 PUBLICATIONS **728** CITATIONS
SEE PROFILE

Angels Gonzalez-Lafont
Autonomous University of Barcelona
119 PUBLICATIONS **1,995** CITATIONS
SEE PROFILE

José M Lluch
Autonomous University of Barcelona
270 PUBLICATIONS **4,290** CITATIONS
SEE PROFILE

Variational Transition-State Theory Rate Constant Calculations of the OH + CH_3SH Reaction and Several Isotopic Variants

Laura Masgrau, Àngels González-Lafont,* and José M. Lluch

Departament de Química, Universitat Autònoma de Barcelona, 08193 Bellaterra, Barcelona. Spain

Received: July 29, 2002; In Final Form: February 12, 2003

In this paper the first variational transition-state theory rate constant calculation for the OH + CH_3SH reaction and several isotopic variants involving OD, CH_3SD, and CD_3SH is presented. Multidimensional tunneling corrections have been included when necessary. The potential energy surface has been described by low-level calculations at the MP2(full)/cc-pVDZ level combined with higher level calculations using the multilevel MCCM-CCSD(T)-CO-2m method. We have found that the reaction takes place by forming first a weakly bound complex that presents two hydrogen bonds between the hydroxyl radical and methanethiol. From this complex two different reaction pathways have been found: abstraction of the hydrogen atom attached to the sulfur atom and abstraction of the hydrogen atom of the methyl group. To take into account the different kinetic channels, the canonical and the competitive canonical unified statistical theories have been used to calculate the global rate constant of the perprotio reaction. Due to the slower nature of the H-abstraction of the methyl group, the global rate constant turns out to be equivalent to the overall rate constant for the abstraction of the hydrogen atom attached to the sulfur atom. It is only at the higher temperature range when a significant percentage of CH_2SH is predicted. An activation energy of −0.54 kcal/mol in the range 225−430 K is obtained for the global reaction, in very good agreement with the experimental results. Several kinetic isotope effects of the global reactions have also been calculated and analyzed in view of previously published experimental results.

1. Introduction

The atmospheric sulfur cycle plays a central role in many adverse effects which may result from sulfur emissions such as acid rain or climate modification. Biological reduction of sulfur compounds is generally believed to be a major natural source of atmospheric sulfur. One of the simplest of all those reduced sulfur compounds is CH_3SH (methanethiol), which accounts for around 10% of the global flux of sulfur compounds.

Atmospheric degradation of reduced sulfur compounds seems to be initiated by reaction with the hydroxyl radical. For this reason, the kinetics of the reaction

$$OH + CH_3SH \rightarrow \text{products} \qquad \text{(R1)}$$

has been the subject of intensive experimental research in the past 25 years. A brief summary of the main kinetic data reported in the literature to date follows.

Atkinson and co-workers[1] studied that reaction in argon at 50−100 Torr over the temperature range 299−426 K by a flash photolysis−resonance fluorescence technique. They obtained an Arrhenius expression of $k(T) = 8.89 \times 10^{-12} \exp[(398 \pm 151)/T]$ cm^3 molecule^{-1} s^{-1}, which implies a small negative activation energy and gives a rate constant at room temperature of $k = (3.39 \pm 0.34) \times 10^{-11}$ cm^3 molecule^{-1} s^{-1}. They suggested that hydrogen atom abstraction may be the major reaction pathway. Using the same technique in argon at 40−120 Torr, Wine and co-workers[2] confirmed those results by obtaining an Arrhenius expression of $k(T) = (1.15 \pm 0.39) \times 10^{-11} \exp[(338 \pm 100)/T]$ cm^3 molecule^{-1} s^{-1} over the temperature range 244−367 K, with a value of $k = (3.37 \pm 0.41) \times 10^{-11}$ cm^3 molecule^{-1} s^{-1} at 298 K. They suggested that a weakly bound $CH_3SH\cdots OH$ complex could be formed prior to the hydrogen atom abstraction. Hatakeyama and Akimoto[3] proposed that the first step of reaction 1 produces that complex or an addition product $CH_3S(OH)H$. Lee and Tang,[4] using the discharge flow−resonance fluorescence technique, obtained a rate constant of $k = (2.56 \pm 0.44) \times 10^{-11}$ cm^3 molecule^{-1} s^{-1} at room temperature below 3 Torr pressure.

On the other hand, an indirect determination of the rate constant of reaction R1 was reported by Cox and Sheppard[5] who, using competitive kinetics techniques, obtained a value about a factor of 3 larger than the ones mentioned above: $k = (9.04 \pm 0.85) \times 10^{-11}$ cm^3 molecule^{-1} s^{-1} at 297 ± 2 K and 1 atm pressure. They suggested that the reaction is enhanced at high pressure and postulated that it proceeds via addition to form an adduct. Hynes and Wine[6a] also studied reaction R1 under atmospheric conditions using a pulsed-laser photolysis−pulsed-laser-induced fluorescence technique at 270 and 300 K. They concluded that all available data in the absence of O_2 support a high-pressure limit value of $k = (3.3 \pm 0.3) \times 10^{-11}$ cm^3 molecule^{-1} s^{-1} at 300 K, with the high-pressure limit being reached at argon pressures of less than 30 Torr. Moreover, they found that CD_3SH reacts with OH 13% slower than CH_3SH, suggesting that abstraction of a methyl hydrogen may be a minor but not totally negligible channel for reaction R1. As the same authors indicate, this result turns out to be somewhat surprising considering that the C−H bonds in CH_3SH are thought to be 6 kcal/mol stronger than the S−H bond. On the other hand, Wine and co-workers[6b] had previously found that CH_3SH and CH_3SD react with OH at identical rates, so these authors deduced that the dominant reaction pathway was addition to the sulfur atom.

10.1021/jp021744x CCC: $25.00
Published on Web 05/09/2003

The first direct measurement of the product yield in the reaction of OH with an organic sulfide was carried out by Tyndall and Ravishankara[7] who, using laser-induced fluorescence, determined that the yield of CH_3S (the product corresponding to the abstraction of the sulfur hydrogen) in reaction R1 was 1.1 ± 0.2. However, this result does not exclude a process involving first the addition product $CH_3S(OH)H$ that would then eliminate H_2O to give CH_3S.

Recently, Butkovskaya and Setser[8] have used an infrared chemiluminiscence method to determine the vibrational distributions of H_2O and HOD molecules formed from the room temperature reactions of OH and OD with CH_3SH for a total pressure of 0.5 Torr. They conclude that the dominant mechanism is attack at the sulfur atom followed by rearrangement to give H_2O (or HOD) from the S−H side of the adduct. Moreover, they estimate the corresponding secondary kinetic isotope effect (KIE) to be $k_{OH}/k_{OD} = 0.68$. In later studies, Butkovskaya and Setser[9] have found that, for a total pressure of 0.5 Torr, the abstraction of a hydrogen atom from the methyl group accounts for 11 ± 2% of the total reaction rate from the OD + CH_3SD reaction and for 24 ± 8% from the OH + CH_3SD reaction. In that work they confirmed the value of 0.67 ± 0.10 for the OH/OD + CH_3SH KIE, whereas the specific OH/OD KIE for the reaction with CH_3SD giving CH_3S turns out to be 0.60 ± 0.05.

In contrast with the experimental effort, from the theoretical side, to our knowledge, only an ab initio study of the reaction R1 exists to date. Wilson and Hirst[10] distinguish between a direct hydrogen atom abstraction from the sulfur atom (that is, without any intermediate along the reaction pathway) and the formation of the addition product $CH_3S(OH)H$. The direct abstraction, highly exothermic ($\Delta H° = -24.7$ kcal/mol) and without enthalpy barrier, would be the major reaction channel. Conversely, the formation of the $CH_3S(OH)H$ adduct turns out to be slightly endothermic (1.4 kcal/mol).

From the results explained above, it can be realized that a number of points still remain unclear. For instance, the way in which the hydrogen abstraction atom from the sulfur end of methanethiol takes place should be clarified: direct abstraction, abstraction through a weakly bound complex, or formation of an addition product prior to the abstraction? In addition, some kinetic isotope effects need further analysis. Then, in this paper we present the first variational transition-state theory rate constant calculations including multidimensional tunneling corrections (when necessary) of the OH + CH_3SH reaction and several isotopic variants, with the aim being to provide a complementary information to the already existing experimental data and to contribute to the understanding of the mechanism and kinetics of that chemical reaction.

2. Method of Calculation

For the electronic structure calculations we used one of the multi-coefficient correlation methods (MCCM) of Truhlar et al.[11−16] This family of methods attempts to extrapolate to the full configuration interaction and to the infinite basis set limits. Particularly, we used the MCCM-CCSD(T) method in its Colorado version and with the 2*m* set of coefficients, which is described elsewhere.[12] In comparison with other high-level electronic methods, the MCCM-CCSD(T) method provides a good compromise between the accuracy of the reaction energy and the energy barriers (see Supporting Information). On the other hand, the MCCM-CCSD(T) method has been proven to give very good rate constants for similar abstraction reactions.[17,18]

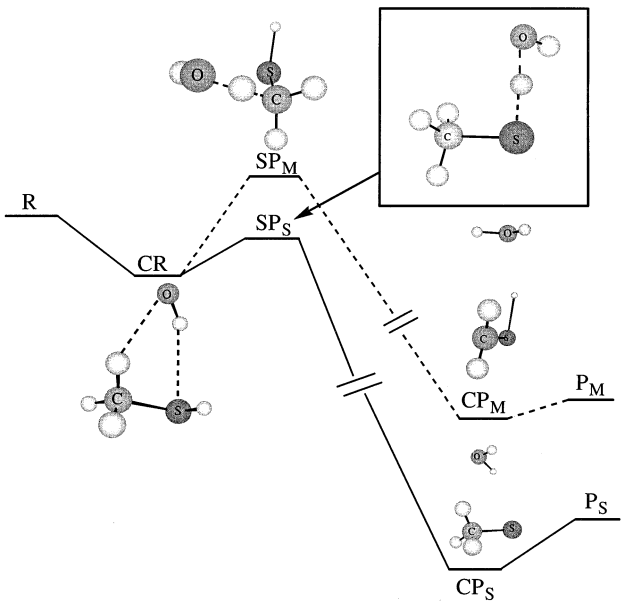

Figure 1. Scheme of the adiabatic ground-state energy (classical potential energy + ZPE corrections) for the OH + CH_3SH reaction. Two different pathways are depicted from the complex in the entrance channel: abstraction of the hydrogen atom bonded to the sulfur atom (solid line) and abstraction of the hydrogen atom from the methyl group (dashed line).

A search for the stationary points involved in the CH_3SH + OH reaction was carried out on the MP2(full)/cc-pVDZ potential energy surface (PES).[19,20] First and second energy derivatives were also calculated at the same level of theory. The reactions were found to occur via the formation of a complex in the entrance channel, which then can lead to two different pathways: the abstraction of the hydrogen atom bonded to the sulfur atom and the H-abstraction from the methyl group (see Figure 1). The association of the reactants takes place without a saddle point, whereas each abstraction has one. The two abstraction pathways also present a complex in their respective product sides. The MCCM-CCSD(T)-CO-2m multilevel energy, used as a high level (HL) in this work, was then evaluated at all the stationary points.

The minimum-energy path (MEP)[21,22] in an isoinertial mass-weighted Cartesian coordinate system was calculated starting from each saddle-point geometry, by following the Page−McIver[23]algorithm at the MP2(full)/cc-pVDZ level of theory. For the H-abstraction from the sulfur atom (we will denote it H_S-abstraction) a step size, δs, of 0.02 bohr was used (*s* denotes the distance along the MEP in an isoinertial mass-scaled coordinate system with a scaling mass equal to 1 amu; $s = 0$ at the saddle point, positive on the product side of the MEP and negative on the reactant side). The HL energy was evaluated at 14 nonstationary points along this MEP. For the H-abstraction from the methyl group (we will call it H_M-abstraction) a step size of 0.01 bohr was used. The HL energy was evaluated at 15 nonstationary points along this MEP. The calculation of the MEPs confirmed that the two abstractions are preceded by the formation of the same complex in the entrance channel.

For the association region, that is the formation of the complex as the reactants approach each other, we have constructed a distinguished reaction coordinate path (DCP) by fixing the intermolecular distance R(C−O) (see Figure 1) and allowing the other degrees of freedom to relax at the MP2(full)/cc-pVDZ level. A total of 11 nonstationary structures, from R(C−O) = 6.97 to 3.67 Å, were calculated, together with their corresponding first and second energy derivatives and their HL

energies. For the dissociations of the product complexes formed after each H abstraction, no DCPs were calculated, as it will be explained below.

For the dynamical calculations the canonical and the competitive canonical unified statistical theories (CUS and CCUS, respectively)[24,25] must be applied because there are several dynamical bottlenecks, both consecutive and competitive. The global rate constant ($k_{R1}(T)$) for the $CH_3SH + OH$ reaction (R1) is then given by

$$\frac{1}{k_{R1}(T)} = \frac{1}{k_{AS}(T)} - \frac{1}{k_{CR}(T)} + \frac{1}{k_S(T) + k_M(T)} \qquad (1)$$

where $k_{AS}(T)$, $k_S(T)$, and $k_M(T)$ are the one-way flux rate constants for the association region, the H_S-abstraction, and the H_M-abstraction, respectively, and $k_{CR}(T)$ is the one-way flux evaluated at the free energy minimum along the reaction path related to the complex formation in the entrance channel. In agreement with the original presentation of CUS theory,[26] the reactant partition function for all these one-way flux rate constants is the same and corresponds to the asymptotic reactants partition function. Note that the dissociations of the product complexes are not taken into account in the evaluation of $k_{R1}(T)$, as they are not expected to have any effect due to the high exothermicity of the reactions. Despite this, the product complexes are included in the calculation of $k_S(T)$ and $k_M(T)$, since their existence modifies the shape of the abstraction-energy profiles.

As mentioned in the Introduction, reaction R1 can be decomposed in two different channels that lead to different products:

$$OH + CH_3SH \rightarrow H_2O + CH_3S \qquad (R1S)$$

$$OH + CH_3SH \rightarrow H_2O + CH_2SH \qquad (R1M)$$

The corresponding rate constants, k_{R1S} and k_{R1M}, are obtained from eqs 2 and 3,[25] respectively:

$$k_{R1S}(T) = \frac{k_S(T)}{k_S(T) + k_M(T)} k_{R1}(T) \qquad (2)$$

$$k_{R1M}(T) = \frac{k_M(T)}{k_S(T) + k_M(T)} k_{R1}(T) \qquad (3)$$

The one-way flux rate constants were evaluated by means of canonical variational transition state theory (CVT),[27−33] plus the small-curvature tunneling (SCT)[34−37] transmission coefficient when necessary.

For the regions with a saddle point (the two H-abstractions), the mapped interpolated scheme for single-point energy corrections (ISPE)[38,39] was used to correct the energetics of the low-level (LL) MEP with the HL energy calculations mentioned above. For the H_S-abstraction, a total of 346 nonstationary points from $s = -3.12$ to $+3.80$ bohr were included in the LL MEP, with the Hessian calculation at every 0.04 bohr. For the H_M-abstraction, the LL MEP consisted of 880 nonstationary points going from $s = -4.99$ to $+3.81$ bohr and with the Hessian calculation at every 0.02 bohr. The fit of the information along the DCP in the association region was done by a Lagrangian interpolation of order 4.

The normal-mode analysis was done in redundant internal coordinates[40] within the harmonic approximation and with a scaling factor of 0.9790 [41] for the vibrational frequencies. The RODS[42] algorithm was applied in order to improve the generalized frequencies along the abstraction MEPs and to get reliable values along the DCP.

The rate constants for the isotopic substituted reactions were calculated following the same procedure, by using the perprotio MEPs and DCP and applying again the RODS algorithm, this time, to account for the isotopic substitution.

The symmetry numbers for each region are calculated according to the expression[43,44] where n stands for the number

$$\sigma(s) = n\sigma^R/\sigma^{GT}(s) \qquad (4)$$

of kinetically equivalent transition states, σ^R is the usual rotational symmetry number for the reactants (or the product of these symmetry numbers if there are two molecular reactants, as in the present case), and $\sigma^{GT}(s)$ corresponds to the usual rotational symmetry number of the generalized transition state at s. In our applications σ^{GT} is independent of s, and thus $\sigma(s)$ becomes a constant σ. In all the cases studied in this paper $\sigma^R = 1$, $\sigma^{GT} = 1$, and $n = 2$, leading to a symmetry number of 2.

The electronic structure calculations for the MEPs were done with the GAUSSRATE8.7 code,[45−47] the DCP and the high-level energies were calculated with GAUSSIAN98,[48] and the rate constants were calculated with POLYRATE8.7.[46]

3. Results and Discussion

In this section we will first present the results for the association region, the H_S-abstraction, the H_M-abstraction, and the global reaction without isotopic substitution. Afterward we will comment on the different kinetic isotope effects obtained.

A. $CH_3SH + OH$ Reaction (R1).

As it has already been introduced, the reactants approach each other to first form a weakly bound complex (CR), which presents two hydrogen bonds (see Figure 1): one between the oxygen atom of the hydroxyl radical and a hydrogen atom of the methyl group of methanethiol, and the other between the hydrogen atom of the hydroxyl radical and the sulfur atom in methanethiol. In the DCP that we have constructed for this association region, the hydroxyl radical does not approach methanethiol keeping the C−S and the O−H bonds parallel, but by the SH-side, with the hydrogen atom of the hydroxyl radical directed to the sulfur atom. As commented, in the CR complex this interaction is still present with a OH···SH distance of 2.53 Å, which is shorter than the H_2CH···OH distance of 2.62 Å. The MCCM-CCSD(T)-CO-2m potential energy at this low-level CR structure is −4.44 kcal/mol (see Table 1). However, the HL minimum along the LL reaction path is found at a structure lying 4.45 kcal/mol below reactants and with OH···SH and H_2CH···OH distances of 2.59 and 3.11 Å, respectively. Although the association presents neither a saddle point nor a maximum in the adiabatic energy profile, it presents a free energy maximum in the temperature range 225−430 K. Therefore, the CVT rate constants for the association can be calculated from 225 to 430 K. As can be seen in Table 2, $k_{AS}(T)$ has a slight dependence on temperature, with values between 5.57×10^{-11} and 5.85×10^{-11} cm^3 molecule^{-1} s^{-1} and with the minimum value at 298−300 K. The one-way flux rate constant value obtained at the free energy minimum corresponding to CR, $k_{CR}(T)$, is also given in Table 2. At 500 K this free energy minimum has disappeared and the free energy maximum in the association region has collapsed to the H-abstraction free energy barrier (see Figure 2). Therefore, at temperatures above 500 K the global rate constant is given solely by the two abstraction processes.

After the CR complex is formed, the reaction can proceed via two different pathways: H_S-abstraction and H_M-abstraction.

TABLE 1: MCCM-CCSD(T)-CO-2m/cc-pVDZ Energetics (kcal/mol) for the Different Regions Described in the OH + CH_3SH Reaction[a]

	ΔV	ΔV_a^G	$V(s=0)$	$s(V_{max})$	V_{max}	$V_a^G(V_{max})$	$s(V^{AG})$	V^{AG}
association	−4.44	−3.10						
H_M-abstraction	−25.53	−24.91	0.74	−0.26	1.41	2.22	−0.35	2.31
M-dissociation	−22.24	−23.00						
H_S-abstraction	−37.44	−34.05	−3.25	−0.37	−2.30	−1.22	−0.50	−1.15
S-dissociation	−33.40	−31.88						

[a] From left to right: classical potential and adiabatic energy of reaction for the region; classical potential energy at the MP2 saddle point structure; *s* value at the classical potential energy maximum; MCCM energy barrier height; adiabatic energy at the classical potential energy maximum; *s* value at the adiabatic energy maximum; adiabatic energy barrier height. All energies are relative to reactants. The *s* values are in bohr.

TABLE 2: Rate Constants (cm^3 $molecule^{-1}$ s^{-1}; power of 10 in parentheses) and Branching Ratio of the Hydrogen Abstraction from the Methyl Group

T(K)	$k_{AS}(T)$	$k_{CR}(T)$	$k_S(T)$	$k_{R1S}(T)$	$k_M(T)$	$k_{R1M}(T)$	$k_{R1}(T)$	% branching[a]
225	5.81(−11)	1.22(−9)	1.73(−11)	1.35(−11)	1.41(−14)	1.10(−14)	1.35(−11)	0.08
244	5.69(−11)	7.23(−10)	1.44(−11)	1.17(−11)	1.81(−14)	1.47(−14)	1.17(−11)	0.13
298	5.57(−11)	2.49(−10)	1.01(−11)	8.85(−12)	3.37(−14)	2.95(−14)	8.88(−12)	0.33
300	5.57(−11)	2.48(−10)	1.00(−11)	8.78(−12)	3.44(−14)	3.02(−14)	8.81(−12)	0.34
350	5.63(−11)	1.28(−10)	8.37(−12)	7.72(−12)	5.51(−14)	5.08(−14)	7.77(−12)	0.65
400	5.75(−11)	8.30(−11)	7.49(−12)	7.20(−12)	8.21(−14)	7.89(−14)	7.28(−12)	1.08
420	5.82(−11)	7.25(−11)	7.32(−12)	7.14(−12)	9.48(−14)	9.25(−14)	7.23(−12)	1.28
430	5.85(−11)	6.82(−11)	7.23(−12)	7.10(−12)	1.02(−13)	1.00(−13)	7.20(−12)	1.39
500			6.96(−12)	6.96(−12)	1.57(−13)	1.57(−13)	7.12(−12)	2.21
600			7.11(−12)	7.11(−12)	2.61(−13)	2.61(−13)	7.37(−12)	3.54
800			8.32(−12)	8.32(−12)	5.73(−13)	5.73(−13)	8.89(−12)	6.45
1000			1.03(−11)	1.03(−11)	1.04(−12)	1.04(−12)	1.13(−11)	9.19

[a] % branching = $(k_{R1M}/(k_{R1S} + k_{R1M})) \times 100$.

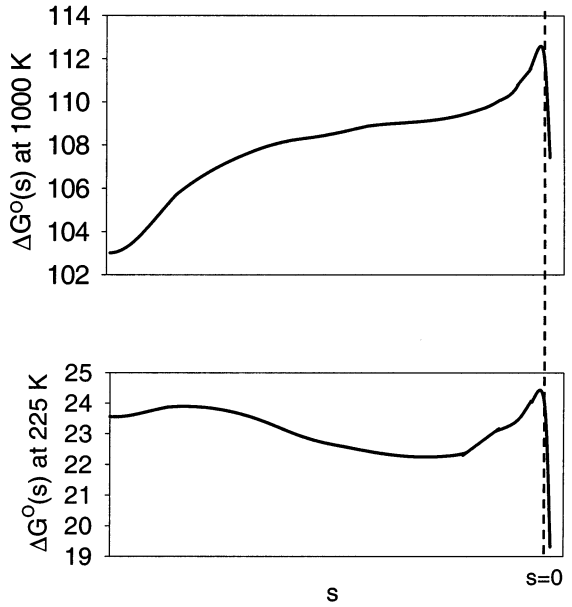

Figure 2. Gibbs free energy curves (kcal/mol) for the overall H_S-abstraction channel (225 and 1000 K) at the association and abstraction regions of the R1 reaction.

The abstraction of the hydrogen atom bonded to the sulfur atom takes place through a LL saddle point structure with a forming and breaking distance of 1.43 and 1.41 Å, respectively. When the HL energy is evaluated along the LL MEP, the classical potential energy maximum (V_{max}) corresponds to a more reactant-like structure (R(O···H) = 1.59 Å and R(S···H) = 1.36 Å), which has a HL energy of −2.30 kcal/mol (see Table 1). At this point it has to be noted that since the adiabatic energy barrier (V^{AG}) is also negative (−1.15 kcal/mol), there will be no tunneling for this H_S-abstraction. In the product side of this channel, a complex is formed by the interaction of the two products with an adiabatic energy of −34.05 kcal/mol (CP_S in Figure 1). The overall HL adiabatic energy of reaction for this pathway (−31.88 kcal/mol) is in very good agreement with the exothermicity value of −32.0 kcal/ mol.[8] In Table 1 it can also be seen that there is a further displacement to reactants of the adiabatic maximum ($s(V^{AG})$) from the HL potential energy maximum ($s(V_{max})$). However, as temperature increases, the variational transition state moves toward products until $s_* = -0.31$ bohr at 1000 K. In any case the variational effects on the H_S-abstraction rate constant are relatively small, with a k^{CVT}/k^{TST} ratio of 0.93 and 0.99 at 225 and 1000 K, respectively, and with no variational effects around 500 K. In the fourth column of Table 2 the CVT rate constants (k_S) for this abstraction region are listed. As a result of the negative barrier, the calculated rate constants are very fast (10^{-11}−10^{-12} cm^3 $molecule^{-1}$ s^{-1}) in the whole range of temperatures studied. Between 225 and 500 K, the H_S-abstraction presents a negative activation energy (E_a) (with a value of −0.77 kcal/mol in the range 225−430 K), which turns out to be positive at temperatures above 500 K. When the association region is taken into account, that is, for the $CH_3SH + OH \rightarrow CR \rightarrow CH_3S + H_2O$ reaction pathway (R1S, see fifth column in Table 2), E_a(225−430 K) slightly changes to −0.56 kcal/mol. The Arrhenius plots for the H_S-abstraction alone (dashed line), k_S, and for the overall H_S-abstraction (solid line), k_{R1S}, are depicted in Figure 3. As it can be seen, the incorporation of the association region below 500 K slightly slows down the rate constants, what provokes a less negative slope.

The other possible reaction pathway after the formation of the CR complex is the abstraction of a hydrogen atom of the methyl group. The overall HL adiabatic energy of reaction for this abstraction (−23.00 kcal/mol) underestimates by 2.7 kcal/mol the proposed exothermicity (−25.7 kcal/mol). As it can be seen in Table 1, the H_M-abstraction is less exothermic than the H_S-abstraction and has a higher barrier height. These results agree with the stronger nature of the C−H bond having to be broken. In the product side of this channel a complex is formed (CP_M) as a result of a hydrogen bond between the O atom of water and the H atom of the SH group in methanethiol. Since

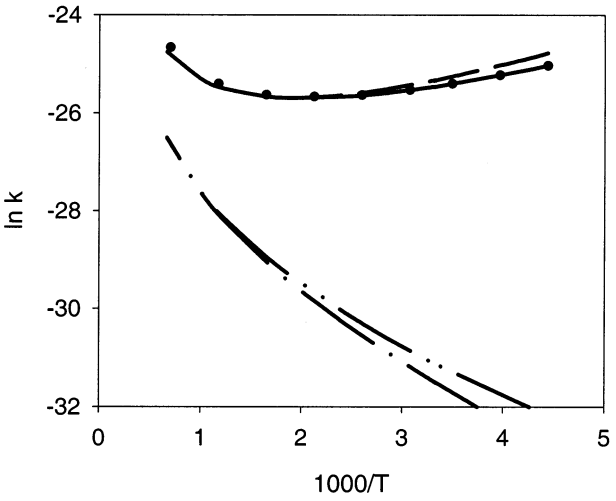

Figure 3. Arrhenius plots for the H_S-abstraction (k_S, dashed line), overall H_S-abstraction (k_{R1S}, solid line), overall H_M-abstraction (k_{R1M}, dashed−dotted−dotted line), and global OH + CH_3SH (k_{R1}, dotted line) reaction rate constants (cm^3 $molecule^{-1}$ s^{-1}). The Arrhenius plot for the CVT rate constant (i.e., without tunneling) for the H_M-abstraction is also shown (dashed−dotted line). Temperatures are given in kelvin.

there is not free rotation around the C−S bond, the hydrogen atoms attached to the carbon atom can be classified into two nonequivalent sets: one hydrogen atom in the trans position with respect to the hydrogen attached to sulfur and the other two hydrogen atoms (we will call them equatorial hydrogens) which are equivalent to each other. For the H_M-abstraction channel we have located a LL saddle point structure (see Figure 1) that leads to the abstraction of one equatorial hydrogen. Since there are two kinetically equivalent saddle points in this case ($n = 2$ in eq 4), the symmetry number turns out to be 2. However, no reaction pathway corresponding to the abstraction of the hydrogen atom in the trans position has been found. In other words, whatever attempt is made to approach the oxygen atom of the OH radical to the hydrogen atom in the trans position leads to the abstraction of an equatorial hydrogen atom. Then only the abstraction of the equatorial hydrogen has to be taken into account in the H_M-abstraction channel. The HL classical potential energy barrier for the H_M-abstraction is 1.41 kcal/mol and increases to 2.31 kcal/mol when the zero-point-energy corrections are added. In Figure 3 the Arrhenius plot for the CVT rate constants for this abstraction is depicted (dashed−dotted line). Since the variational effects for this abstraction are relatively small (0.83 and 1.00 at 225 and 1000 K, respectively), the TST Arrhenius plot would be very similar to the CVT one. Despite the low adiabatic barrier height, tunneling effects are noticeable and increase the rate constant by a factor of 2.55 at 225 K and 1.11 at 600 K. The CVT/SCT rate constants ($k_M(T)$) are given in the sixth column of Table 2. They go from $\sim 10^{-14}$ to $\sim 10^{-12}$ cm^3 $molecule^{-1}$ s^{-1}, which are 2 or 3 orders of magnitude smaller than the association ones. Therefore, the rate constants for the overall H_M-abstraction ($k_{R1M}(T)$) are very close to $k_M(T)$ in the whole range of temperatures. The corresponding Arrhenius plot is also depicted in Figure 3 (dashed−dotted−dotted line).

Due to the slower nature of the H_M-abstraction, when the global reaction rate constant for the methanethiol + OH reaction (R1) is calculated by eq 1, it turns out to be practically the one corresponding to the overall H_S-abstraction (R1S). As it can be seen in Figure 3 (dotted line) and in the last column of Table 2, only at high temperatures does the H_M-abstraction channel have a significant contribution. This fact confirms the results

TABLE 3: k_{R1}/k_{Ri} ($i = 2-6$) Kinetic Isotope Effects

T (K)	R2	R3	R4	R5	R6
225	1.40	0.99	0.85	1.17	0.85
244	1.40	0.99	0.87	1.19	0.86
298	1.41	1.00	0.90	1.25	0.90
300	1.41	1.00	0.90	1.25	0.90
350	1.41	1.00	0.93	1.29	0.92
400	1.40	1.00	0.94	1.30	0.93
420	1.40	1.00	0.94	1.31	0.94
430	1.40	1.00	0.94	1.31	0.94
500	1.37	1.00	0.95	1.31	0.95
600	1.36	1.00	0.97	1.31	0.97
800	1.32	1.01	0.98	1.30	0.99
1000	1.29	1.01	0.99	1.28	1.00

TABLE 4: k_{R1S}/k_{RiS} ($i = 2-6$) Kinetic Isotope Effects

T (K)	R2S	R3S	R4S	R5S	R6S
225	1.40	0.99	0.85	1.17	0.85
244	1.40	0.99	0.87	1.20	0.86
298	1.41	0.99	0.90	1.25	0.90
300	1.41	0.99	0.90	1.25	0.90
350	1.41	0.99	0.93	1.29	0.92
400	1.41	0.99	0.94	1.31	0.93
420	1.41	0.99	0.94	1.32	0.94
430	1.41	0.99	0.94	1.32	0.94
500	1.39	1.00	0.95	1.32	0.95
600	1.38	1.00	0.97	1.33	0.96
800	1.36	1.00	0.98	1.33	0.98
1000	1.34	1.00	0.99	1.32	0.98

of Tyndall and Ravishankara[7] who showed that the CH_3S yield for reaction R1 was unity. Interestingly, the calculated branching ratio of the hydrogen abstraction from the methyl group at high temperatures approaches the values measured by Butkovskaya and Setser[9] from the infrared chemiluminiscent spectra of the water (or deuterated water) formed in the reaction. The global rate constants obtained in this work for the low-pressure limit for the perprotio reaction (k_{R1}, eighth column of Table 2) turn out to be 3−4 times smaller than the high-pressure experimental values in the range where experimental data are available (244−426 K). The calculated activation energy for the R1 reaction between 225 and 430 K (−0.54 kcal/mol) is in very good agreement with the experimental value of -0.7 ± 0.2 kcal/mol.

B. Kinetic Isotope Effects. We have studied the following isotopic variants of reaction R1:

$$OH + CH_3SD \rightarrow \text{products} \quad \text{(R2)}$$

$$OH + CD_3SH \rightarrow \text{products} \quad \text{(R3)}$$

$$OD + CH_3SH \rightarrow \text{products} \quad \text{(R4)}$$

$$OD + CH_3SD \rightarrow \text{products} \quad \text{(R5)}$$

$$OD + CD_3SH \rightarrow \text{products} \quad \text{(R6)}$$

Similarly to the case of reaction R1, each one of these global reactions Ri ($i = 2-6$) can be split into reactions RiS and RiM ($i = 2-6$), depending on which is the atom that is abstracted: the hydrogen (or deuterium) attached to the sulfur or to the methyl group, respectively. k_{Ri}, k_{RiS}, and k_{RiM} ($i = 2-6$) stand for the corresponding rate constants. From them the KIEs k_{R1}/k_{Ri}, k_{R1S}/k_{RiS}, and k_{R1M}/k_{RiM} ($i = 2-6$) are presented in Tables 3−5, respectively.

It can be seen that, due to the fact that the H_S-abstraction (or D_S-abstraction) channel is clearly faster than the corresponding H_M-abstraction (or D_M-abstraction) channel, the KIEs of each

TABLE 5. k_{R1M}/k_{RiM} ($i = 2-6$) Kinetic Isotope Effects

T (K)	R2M	R3M	R4M	R5M	R6M
225	0.88	1.81	0.82	0.74	1.52
244	0.89	1.73	0.82	0.76	1.48
298	0.92	1.59	0.85	0.82	1.42
300	0.92	1.58	0.85	0.82	1.41
350	0.93	1.50	0.88	0.85	1.38
400	0.95	1.44	0.90	0.89	1.35
420	0.95	1.44	0.90	0.90	1.34
430	0.96	1.44	0.91	0.90	1.34
500	0.96	1.39	0.92	0.92	1.33
600	0.97	1.33	0.95	0.95	1.31
800	0.98	1.26	0.98	0.98	1.26
1000	0.99	1.25	1.00	1.00	1.26

global reaction Ri are essentially determined by the KIEs of the reaction RiS, the RiM reaction having only a small effect at high temperatures. Reaction R2 shows a small inverse secondary KIE for the H_M-abstraction channel but a clear normal primary KIE for the D_S-abstraction channel and the global reaction. This result contrasts with the experiments of Wine and co-workers[6b] who found that CH_3SH and CH_3SD react with OH at identical rates, so these authors deduced that the dominant reaction pathway is addition to the sulfur atom. From our calculations we discard the formation of the $CH_3S(OH)H$ adduct: In our PES we have not found any reaction path that leads to that adduct. Anyway, it has to be noted that the formation of this $CH_3S(OH)H$ adduct on the PES built up by Wilson and Hirst[10] was endothermic, for which this addition process would be highly unfavored versus the H_S-abstraction channel through the weakly bound complex CR. However, we cannot exclude that our calculated KIE for reaction R2 could be wrong. This KIE at 298 K comes from the free energy barrier that exists in the H_S-abstraction (or D_S-abstraction) region, which is clearly higher than the free energy barrier in the association region. However, as temperature decreases, the positive entropic contribution ($-T\Delta S$) to that H_S-abstraction (or D_S-abstraction) free energy barrier diminishes, so increasing the corresponding k_S rate constant (see the fourth column in Table 2). We have found that between 100 and 150 K k_{AS} already becomes smaller than k_S, thus dominating the reaction rate of this channel at these temperatures. Since the free energy barrier of the association region appears very early, it is not able to discriminate between CH_3SH and CH_3SD. So, our calculations predict no significant KIE between 100 and 150 K or below. This way the discrepancy with the experimental measurements of Wine and co-workers[6b] would focus merely on the range of temperature in which no significant KIE exists for reaction R2. In this sense, we have calculated that a reduction of about 1 kcal/mol in the free energy barrier of the H_S-abstraction (or D_S-abstraction) region would equal the rate constants k_S and k_{AS} already at room temperature. In this scenario, no significant KIE at 298 K would be theoretically predicted in good agreement with the experimental results. It has to be emphasized that, at the present state-of-the-art of electronic and dynamical calculations, we cannot exclude an error of 1 kcal/mol in the free energy barrier (which depends on the enthalpic term, the entropic contribution, and the variational effect). However, at least, we have demonstrated that the abstraction of the hydrogen/deuterium atom attached to the sulfur atom through a weakly bound complex (CR) is compatible with the absence of a primary KIE for the R2 reaction, the formation of any $CH_3S(OH)H$ adduct not being required.

Reaction R3 shows a normal primary KIE for the D_M-abstraction channel but practically no KIE for the H_S-abstraction channel and the global reaction. Again, our theoretical result introduces some discrepancy with the experiments of Hynes and Wine[6a] who found that CD_3SH reacts with OH 13% slower than CH_3SH. This time, we think that our theoretical results are right because any KIE for this reaction would come from the H_M-abstraction (or D_M-abstraction) channel, which proceeds too slowly to be able to contribute significantly to the global reaction, except at high temperatures. This conclusion is reinforced from the knowledge of the dissociation energies D_0 corresponding to the S−H and C−H bonds in CH_3SH that turn out to be 86.1 ± 0.5 and 92.4 ± 2.0 kcal/mol, respectively.[49] Since the tunneling effect for the H_M-abstraction (or D_M-abstraction) channel is unable to compensate for such a difference, the contribution of the H_M-abstraction (or D_M-abstraction) channel turns out to be practically negligible.

Reaction R4 exhibits an inverse secondary KIE for both abstraction channels and for the global reaction. Reaction R5 also shows an inverse secondary KIE for the H_M-abstraction channel, but a normal KIE resulting from a primary plus a secondary contribution for both the D_S-abstraction channel and the global reaction. Finally, reaction R6 presents a normal KIE resulting from a primary plus a secondary contribution for the D_M-abstraction channel and an inverse secondary KIE for both the H_S -abstraction channel and the global reaction.

4. Conclusions

In this paper we have carried out the first variational transition-state theory rate constant calculations with multidimensional tunneling corrections (when necessary) of the OH + CH_3SH reaction and several isotopic variants involving OD, CH_3SD, and CD_3SH. We have found that the reaction takes place by forming first a weakly bound complex that presents two hydrogen bonds between the hydroxyl radical and methanethiol. From this complex two reaction paths diverge, one leading to the abstraction of the hydrogen atom attached to the sulfur atom and the other one consisting of the hydrogen abstraction of the methyl group. The first channel proceeds much faster than the second one, in such a way that the CH_3S product is obtained almost exclusively, except at high temperatures where a significant percentage of CH_2SH is predicted. An activation energy of −0.54 kcal/mol in the range of 225−430 K is obtained for the global reaction, in very good agreement with the experimental results. A positive activation energy is found at temperatures above 500 K. The kinetic isotope effects of the global reactions are essentially determined by the channel corresponding to the abstraction of the hydrogen (or deuterium) attached to the sulfur. Our calculations predict some OH + CH_3SH/CH_3SD KIE above 150 K (although a reduction of only 1 kcal/mol in the free energy barrier of the abstraction of the hydrogen attached to sulfur would delay a significant appearance of this KIE up to above room temperature), but no OH + CH_3SH/CD_3SH KIE.

Finally, it has to be mentioned that the calculations presented in this work are for the low-pressure limit of the reaction, while some of the experimental rate constants correspond to the high-pressure limit. This fact could explain some differences between computed and experimental results.

Acknowledgment. Financial support from the DGESIC through Project PB98-0915 and the use of the computational facilities of the CESCA are gratefully acknowledged.

Supporting Information Available: Energetics for the R1M and R1S channels at different electronic levels of calculation (Table 1S) and Cartesian coordinates of the MP2(full)/cc-pVDZ

stationary-point structures (Table 2S). This material is available free of charge via the Internet at http://pubs.acs.org.

References and Notes

(1) Atkinson, R.; Perry, R. A.; Pitts, J. N., Jr. *J. Chem. Phys.* **1977**, *66*, 1578.

(2) Wine, P. H.; Kreutter, N. M.; Gump, C. A.; Ravishankara, A. R. *J. Phys. Chem.* **1981**, *85*, 2660.

(3) Hatakeyama, S.; Akimoto, H. *J. Phys. Chem.* **1983**, *87*, 2387.

(4) Lee, J. H.; Tang, I. N. *J. Chem. Phys.* **1983**, *78*, 6646.

(5) Cox, R. A.; Sheppard, D. *Nature (London)* **1980**, *284*, 330.

(6) (a) Hynes, A. J.; Wine, P. H. *J. Phys. Chem.* **1987**, *91*, 3672. (b) Wine, P. H.; Thompson, R. J.; Semmes, D. H. *Int. J. Chem. Kinet.* **1984**, *16*, 1623.

(7) Tindall, G. S.; Ravishankara, A. R. *J. Phys. Chem.* **1989**, *93*, 4707.

(8) Butkovskaya, N. I.; Setser, D. W. *J. Phys. Chem. A* **1998**, *102*, 6395.

(9) Butkovskaya, N. I.; Setser, D. W. *J. Phys. Chem. A* **1999**, *103*, 6921.

(10) Wilson, C.; Hirst, D. M. *J. Chem. Soc., Faraday Trans.* **1995**, *91*, 3783.

(11) Tratz, C. M.; Fast, P. L.; Truhlar, D. G. *Phys. Chem. Commun.* **1999**, *2* (14), 1.

(12) Fast, P. L.; Corchado, J. C.; Sánchez, M. L.; Truhlar, D. G. *J. Phys. Chem. A* **1999**, *103*, 5129.

(13) Fast, P. L.; Sánchez, M. L.; Corchado, J. C., Truhlar, D. G. *J. Chem. Phys.* **1999**, *110*, 11679.

(14) Fast, P. L.; Sánchez, M. L.; Truhlar, D. G. *Chem. Phys. Lett.* **1999**, *306*, 407.

(15) Fast, P. L.; Truhlar, D. G. *J. Phys. Chem. A* **2000**, *104*, 6111.

(16) Fast, P. L.; Schultz, N. E.; Truhlar, D. G. *J. Phys. Chem. A* **2001**, *105*, 4143.

(17) Masgrau, L.; González-Lafont, A.; Lluch J. M. *J. Chem. Phys.* **2001**, *115*, 4515.

(18) Masgrau, L.; González-Lafont, A.; Lluch J. M. *Theor. Chem. Acc.* **2002**, *107*, 147.

(19) Dunning, T. H., Jr. *J. Chem. Phys.* **1989**, *90*, 1007.

(20) Woon, D. E.; Dunning, T. H., Jr. *J. Chem. Phys.* **1995**, *103*, 4572.

(21) Truhlar, D. G.; Kupperman, A. *J. Am. Chem. Soc.* **1971**, *93*, 1840.

(22) Fukui, K. *Pure Appl. Chem.* **1982**, *54*, 1825.

(23) Page, M.; McIver, J. W., Jr. *J. Chem. Phys.* **1988**, *88*, 922.

(24) Hu, W.-P.; Truhlar, D. G. *J. Am. Chem. Soc.* **1995**, *117*, 10726.

(25) Hu, W.-P.; Truhlar, D. G. *J. Am. Chem. Soc.* **1996**, *118*, 860.

(26) Garrett, B. C.; Truhlar, D. G. *J. Chem. Phys.* **1982**, *76*, 1853.

(27) Garrett, B. C.; Truhlar, D. G. *J. Chem. Phys.* **1979**, *70*, 1593.

(28) Garrett, B. C.; Truhlar, D. G. *J. Phys. Chem.* **1979**, *83*, 1079.

(29) Garrett, B. C.; Truhlar, D. G. *J. Am. Chem. Soc.* **1979**, *101*, 4534.

(30) Garrett, B. C.; Truhlar, D. G. *J. Am. Chem. Soc.* **1979**, *101*, 5207.

(31) Garrett, B. C.; Truhlar, D. G.; Grev, R. S.; Magnuson, A. W. *J. Phys. Chem.* **1980**, *84*, 1730. Erratum: Garrett, B. C.; Truhlar, D. G.; Grev, R. S.; Magnuson, A. W. *J. Phys. Chem.* **1983**, *87*, 4554.

(32) Isaacson, A. D.; Truhlar, D. G. *J. Chem. Phys.* **1982**, *76*, 1380.

(33) Truhlar, D. G.; Isaacson, A. D.; Garrett, B. C. In *Theory of Chemical Reaction Dynamics*; Baer, M., Ed.; CRC Press: Boca Raton, FL, 1985; Vol. 4, pp 65−137.

(34) Liu, Y.-P.; Lynch, G. C.; Truong, T. N.; Lu, D.-h.; Truhlar, D. G.; Garrett, B. C. *J. Am. Chem. Soc.* **1993**, *115*, 2408.

(35) Lu, D.-H.; Truong, T. N.; Melissas, V.; Lynch, G. C.; Liu, Y.-P.; Garrett, B. C.; Steckler, R.; Isaacson, A. D.; Rai, S. N.; Hancock, G. C.; Laurderdale, J. G.; Joseph, T.; Truhlar, D. G. *Comput. Phys. Commun.* **1992**, *71*, 235.

(36) Truhlar, D. G.; Gordon, M. S. *Science* **1990**, *249*, 491.

(37) Truong, T. N.; Lu, D.-H.; Lynch, G. C.; Liu, Y.-P.; Melissas, V.; Stewart, J. J. P.; Steckler, R.; Garrett, B. C.; Isaacson, A. D.; González-Lafont, A.; Rai, S. N.; Hancock, G. C.; Joseph, T.; Truhlar, D. G. *Comput. Phys. Commun.* **1993**, *75*, 143.

(38) Corchado, J. C.; Coitiño, E. L.; Chuang, Y.-Y.; Fast, P. L.; Truhlar, D. G. *J. Phys. Chem.* **1998**, *102*, 2424.

(39) Chuang, Y.-Y.; Corchado, J. C.; Truhlar, D. G. *J. Phys. Chem. A* **1999**, *103*, 1140.

(40) Chuang, Y.-Y.; Truhlar, D. G. *J. Phys. Chem. A* **1998**, *102*, 242.

(41) Fast, P. L.; Corchado, J. C.; Sánchez, M. L.; Truhlar, D. G. *J. Phys. Chem. A* **1999**, *103*, 3139.

(42) Villà, J.; Truhlar, D. G. *Chem. Theor. Acc.* **1997**, *97*, 317.

(43) Villà, J.; Corchado, J. C.; González-Lafont, A.; Lluch, J. M.; Truhlar, D. G. *J. Phys. Chem. A* **1999**, *103*, 5061.

(44) Masgrau, L.; González-Lafont, A.; Lluch, J. M. *J. Chem. Phys.* **2001**, *114*, 2154.

(45) Corchado, J. C.; Chuang, Y.-Y.; Coitiño, E. L.; Truhlar, D. G. *Gaussrate 8.7*; University of Minnesota: Minneapolis, 2001 (based on Polyrate 8.7 [46] and Gaussian 94 [47]) (http://comp.chem.umn.edu/polyrate).

(46) Corchado, J. C.; Chuang, Y.-Y.; Fast, P. L.; Villà, J.; Hu, W.-P.; Liu, Y.-P.; Lynch, G. C.; Nguyen, K. A.; Jackels, C. F.; Melissas, V.; Lynch, B. J.; Rossi, I.; Coitiño, E. L.; Fernández-Ramos, A.; Pu, J.; Steckler, R.; Garrett, B. C.; Isaacson, A. D.; Truhlar, D. G. *Polyrate 8.7*; University of Minnesota: Minneapolis, 2001 (http://comp.chem.umn.edu/polyrate).

(47) Frisch, M. J.; Trucks, G. W.; Schlegel, H. B.; Gill, P. M. W.; Johnson, B. G.; Robb, M. A.; Cheeseman, J. R.; Keith, T. A.; Petersson, G. A.; Montgomery, M. A.; Raghavachari, K.; Al-Laham, M. A.; Zakrzewski, V. G.; Ortiz, J. V.; Foresman, J. B.; Cioslowski, J.; Stefanov, B. B.; Nanayakkara, A.; Challacombe, M.; Peng, C. Y.; Ayala, P. Y.; Chen, W.; Wong, M. W.; Andres, J. L.; Replogle, E. S.; Gomperts, R.; Martin, R. L.; Fox, D. J.; Binkley, J. S.; Defrees, D. J.; Baker, J.; Stewart, J. P.; Head-Gordon, M.; Gonzalez, C.; Pople, J. A. *Gaussian 94*; Gaussian Inc.: Pittsburgh, PA, 1995.

(48) Frisch, M. J.; Trucks, G. W.; Schlegel, H. B.; Scuseria, G. E.; Robb, M. A.; Cheeseman, J. R.; Zakrzewski, V. G.; Montgomery, J. A.; Stratmann, R. E.; Burant, J. C.; Dapprich, S.; Millam, J. M.; Daniels, A. D.; Kudin, K. N.; Strain, M. C.; Farkas, O.; Tomasi, J.; Barone, V.; Cossi, M.; Cammi, R.; Mennucci, B.; Pomelli, C.; Adamo, C.; Clifford, S.; Ochterski, J.; Petersson, G. A.; Ayala, P. Y.; Cui, Q.; Morokuma, K.; Malick, D. K.; Rabuck, A. D.; Raghavachari, K.; Foresman, J. B.; Cioslowski, J.; Ortiz, J. V.; Stefanov, B. B.; Liu, G.; Liashenko, A.; Piskorz, P.; Kamaromi, I.; Gomperts, R.; Martin, R. L.; Fox, D. J.; Keith, T.; Al-Laham, M. A.; Peng, C. Y.; Nanayakkara, A.; Gonzalez, C.; Challacombe, M.; Gill, P. M. W.; Johnson, B. G.; Chen, W.; Wong, M. W.; Andres, J. L.; Head-Gordon, M.; Replogle, E. S.; Pople, J. A. *Gaussian 98*; Gaussian Inc.: Pittsburgh, PA, 1998.

(49) Berkowitz, J.; Ellison, G. B.; Gutman, D. *J. Phys. Chem.* **1994**, *98*, 2744.